Simulation of free surface and molten metal behavior during induction melting of an aluminium alloy

A Bansal, P Chapelle, E Waz, Y Delannoy, P Le Brun, J.P. Bellot

Simulation of free surface and molten metal behavior during induction melting of an aluminium alloy

A. Bansal[1], P. Chapelle[1], E. Waz[2], Y. Delannoy[3], P. Le Brun[2] and J.P. Bellot[1]

[1] Institut Jean Lamour, UMR 7198, Université de Lorraine/CNRS - LabEx DAMAS, CS 50840, 54011 Nancy, France

[2] Constellium Technology Center, CS 10027, 38341 Voreppe Cedex, France

[3] SIMaP, Grenoble-INP, UJF, CNRS, BP 75, 38402 St. Martin d'Hères, France

Corresponding author: emmanuel.waz@constellium.com

Abstract

Electromagnetic forces are widely used for processing metal alloys in particular in the aluminium casting industry. Induction is used in melting technologies (both crucible and channel induction furnaces). Magnetic stirrers are also used in melting or casting furnaces. However these technologies applied to opaque melts require modelling to be done to understand the resultant impact on the fluid and improve the process control. This is especially the case of crucible induction furnaces. A 2D axially symmetric numerical model describing the coupled magnetohydrodynamic and free surface phenomena taking place in an induction metal bath has been developed. The model uses the Ansys Fluent software, supplemented with additional User Defined Functions for the calculation of the Lorentz forces acting on the metal. The calculation of the shape of the free surface is based on the Volume Of Fluid method and a RANS k-ω Shear Stress Transport (SST) approach is used to describe the turbulent stirring of the metal. An original feature of our model is the consideration of an oxide skin covering the metal free surface. It was considered that the oxide film behaves similarly to a deforming wall and that friction effects between the oxide film and the metal result in the development of a shear stress at the top surface of the melt. Two examples of application of model are reported, for lab scale and industrial scale induction furnaces. The lab scale results are compared with measurements of the free surface shape obtained using a fringe projection technique.

Key words: Induction Melting, Aluminum Bath, Free Surface Deformation, Measurement, Simulation

Introduction

Electromagnetic forces are widely used in molten metal production, including aluminium cast houses. These forces can be very powerful and provide means for non-contact actions on the very corrosive molten aluminium. Electromagnetic forces are used for induction melting of aluminium, in particular for scrap melting [1]. In this application, a molten heel is often used and the turbulence generated by the electromagnetic field enhances the immersion of the solid in the liquid metal. This, together with the absence of gas burners, reduces the oxidation of the scrap prior to remelt and after the solid has been molten. Electromagnetic forces are frequently used to stir aluminium furnaces. Different technologies exist: side stirrers can be installed on most furnaces while bottom stirrers are limited to tilting furnaces. Stirrers can provide several benefits, including the thermal homogenization of the metal bath, an enhanced melt rate, significant energy savings, an improved alloying efficiency and even a reduction in dross generation [2]. Transport ladles can also be stirred by the same process, avoiding thermal gradient and reducing dross generation [3]. Other applications of electromagnetic forces are considered for molten aluminium filtration. Lorentz forces are studied for the separation of non-metallic inclusions in a molten aluminium flow by electromagnetophoresys [4, 5]. It has also been discovered that priming of ceramic foam filters may be significantly enhanced when Lorentz forces are applied [6]. This allows finer or thicker filters to be used for aluminium production and hence an increased metal quality to be expected. Electromagnetic forces are also used to lift the metal: electromagnetic pumps and rising launders [7].

The effect of electromagnetic forces depends on several parameters. Therefore modelling is desired to define the correct equipment or to set operational parameters. This paper reports the development of a model to describe the hydrodynamics of molten aluminium in a coreless induction furnace.

Numerical model

The induction furnace is axisymmetric except its helical coil, but to simplify our model the coil is described as a hollow cylinder with vertical axis (x-direction of the model), and its meridional section (rectangle in the x-r plane) is crossed by a current density in the direction. Also, it was considered that the temperature in the stirred metal bath was homogeneous and thus the energy equation was not solved. Our model is then 2D axisymmetric and includes the induction phenomena: the turbulent liquid metal flow inside the crucible, the deformation of the free surface of the

metal bath and the presence of an oxide layer covering the metal bath.
The electromagnetic problem is solved using the harmonic A-V formulation, with an imposed current density $\boldsymbol{jc}(t)$ in the coil. Using the hypothesis of axisymmetry, the electric current $\boldsymbol{j}$ and the vector potential $\boldsymbol{A}$ have only one component, along θ, so that there is no need for an electrical potential V to close the current loops, except in the coil where a gradient $\boldsymbol{\nabla} V$ of electric potential is present in the θ direction. The magnetic field $\boldsymbol{B}=\nabla\times\boldsymbol{A}$ is contained in the x-r plane as the velocity $\boldsymbol{U}$ of the liquid metal, and the current density can be written from the Ohm's law, using the electric conductivity σ_e:

$$\boldsymbol{j}=\sigma_e(-\boldsymbol{\nabla} V+\boldsymbol{U}\times\boldsymbol{B}-\partial\boldsymbol{A}/\partial t) \quad (1)$$

The magnetic vector potential A is the solution of a transport equation (coming from the Ohm's law, the Maxwell-Ampere equation $\nabla\times B=\mu_0 j$ where μ_0 is the magnetic permeability of void, and a gauge condition $\nabla\cdot A=0$). Here, j, B, A and V are harmonic and we use their phasors or phasors of their components in (x,r,θ) coordinates. The transport equation for A_θ, and the θ–component of the ohm's law then become:

$$-\nabla\cdot(\nabla A_\theta)=\mu_0 j_\theta-\frac{A_\theta}{r^2} \text{ where } j_\theta=\sigma_e\left(-\frac{\partial V}{r\partial\theta}+U_x B_r-U_r B_x-i\omega\omega_\theta\right) \quad (2)$$

Here, $i=\sqrt{-1}$ and ω is the pulsation of electromagnetic fields. This complex transport equation is solved in the whole domain, including a part of atmosphere big enough to enable the magnetic lines to close freely (chosen here as ten times the coil size in both directions), with boundary conditions $A_\theta=0$ on its outer surface and $\partial A_\theta/\partial r=0$ on its axis. A_θ and its derivatives are continuous at internal boundaries between materials, because there is no ferromagnetic material, and the source term $\mu_0\sigma\partial V/r\partial\theta$ is zero except in the coil, where the Ohm's law is replaced by an imposed current density, uniform in the rectangular section of the coil.
The induction equations (real and imaginary parts of eqn. 2) are implemented in the commercial software Ansys/Fluent13, using user-defined scalar transport equations, and used since several years [8]. The solution $A_\theta(x,r)$ is used to calculate the current density (eqn 1), the electromagnetic force $f=j\times B$ per unit volume, which is not harmonic, but as product of two harmonic functions, it has a mean part $f=\mathrm{Re}(j\times B^*)/2$, where * is the complex conjugate and Re() the real part. The fluctuating part of f is not taken into account because of the inertia of the fluid.
Standard models contained in Ansys/Fluent® are used to describe the fluid flow (Reynolds-Averaged Navier-Stokes equations, with f as a source term), the turbulent friction (k-ω SST model for turbulence) and the deformation of the free surface, using a VOF method (Volume Of Fluid) with a geometric reconstruction.
The oxide layer which covers the free surface of the metal bath is considered homogeneous, and impacts both the surface tension σ of the metal, and the friction $\boldsymbol{\tau}$ of the fluid on the interface. Volumetric forces are present in the Fluent VOF model to represent the surface tension, and the value of σ has been adjusted to represent the oxide layer. However, friction had to be added using a volumetric force proportional to the fluid velocity, because the oxide is supposed fixed:

$$\vec{F}_{vol}=\vec{\tau}_{oxide}\,A=-C_f A\left(\vec{V}_m.\vec{t}\right)\vec{t} \quad (3)$$

Where C_f is a friction coefficient, A is the interfacial area density and $\boldsymbol{t}$ is the unit vector tangent to the interface. Numerical tests on C_f [9] have shown that its precise value is not important.

Lab scale induction furnace

The numerical model was applied to simulate a series of experiments performed in a laboratory scale induction furnace using a 4 kg molten metal bath of aluminium alloy Al-1xxx series. The melt was contained in a 106 mm internal diameter alumina crucible, which was placed in a 8 turn coil operated with a fixed frequency of 3.5 kHz and a current ranging from 1000 A to 3000 A. Since the furnace was operated under atmospheric conditions, the free surface of the melt was instantaneously covered by a uniform oxide layer. During an experiment, the profile of the free surface was measured using a fringe projection technique. As shown in Fig. 1, this technique consists of projecting a fringe line pattern onto the surface and recording the deformed pattern reflected from the surface using one or two camera. The processing of the recorded surface image, together with the principle of triangulation, enables to determine the absolute height of any point of the surface, from which it is possible to reconstruct the 3D profile of the free surface. In this paper, we present measurements carried out by projecting and processing a sequence of patterns (combining a phase shift method with gray coding) in order to achieve a better spatial resolution and by observing the surface using two cameras so as to minimize shadow regions. The spatial and temporal resolutions with this method were typically ± 0.1 mm and 0.03 Hz.
The series of measurements performed has shown that the free surface has a classical dome type shape, exhibiting only small deviation from cylindrical symmetry and relatively modest temporal oscillations with a maximum amplitude of about 4 mm. As expected, the dome height was found to increase with the coil current. Fig. 2 presents a comparison between the measured and computed profiles of the free surface in the case of a coil current intensity of 1507 A. The

figure displays steady state simulation results obtained without considering the free surface oxidation and with the addition of a friction force at the free surface modelling the presence of an oxide film covering the melt.

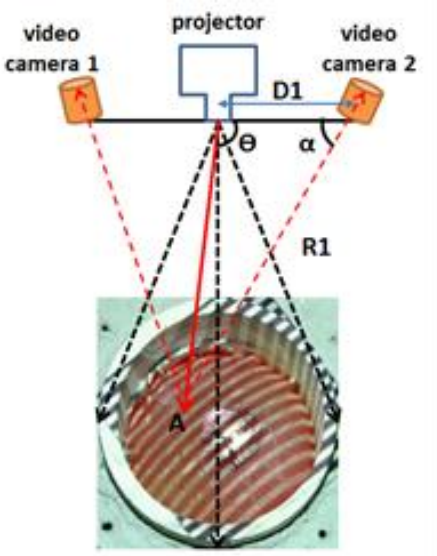

Fig. 1: Sketch of the measurement method of the free surface profile using a structured light projection technique.

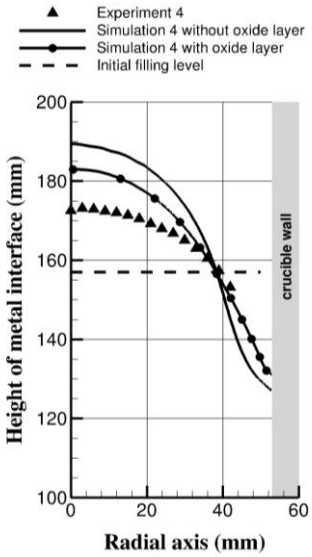

Fig. 2: Comparison between the measured and calculated free surface dome profiles with/without surface oxidation.

The density, dynamic viscosity, electrical conductivity and surface tension of the liquid metal were taken equal to 2379 $kg.m^{-3}$, $1.15x10^{-3}$ Pa.s, $3.97x10^{6}$ $\Omega^{-1}.m^{-1}$ and 0.865 $N.m^{-1}$ respectively. The amplitude of the deformation of the free surface is observed to be considerably reduced by the surface oxidation. Without oxidation, the maximum height of the interface at the axis is 190 mm while the dome height is 62 mm. In the presence of the oxide film, the height of the interface reduces by almost 7 mm along the axis. Note that it was also noticed that the friction force exerted by the oxide film modifies the fluid flow, especially in the upper dome region (the average velocity was reduced by about 30 %) and that the turbulent intensity was as a consequence comparatively much lower in the dome region. As shown in Fig. 2, compared to the measurements, the profile obtained taking into account the friction force due to the oxide film is much closer to the measured profile, although some discrepancies still remain. As discussed in a previous paper [9], the discrepancy between the measured and the calculated dome profiles can most likely be attributed at least partly, if not totally, to the approximation made in the representation of the inductor setup in the numerical model (the disjointed 8 turn coil was represented as continuous sheet of current). Other reasons such as the variation of the alloy properties with the bath temperature and the modelling of the damping of turbulence near the free surface were also investigated and were found to be inconsequential with respect to the bath free surface deformation.

Industrial scale induction furnace

The numerical model was applied to simulate a series of experiments performed in an industrial scale induction furnace using a 5 tons molten metal bath of aluminium alloy Al-2xxx series. In this paper, two extreme operating conditions that correspond to very different numerical cases, useful to validate the model on an industrial scale were observed experimentally and modeled. The inductor works in both cases at full power at low frequency.

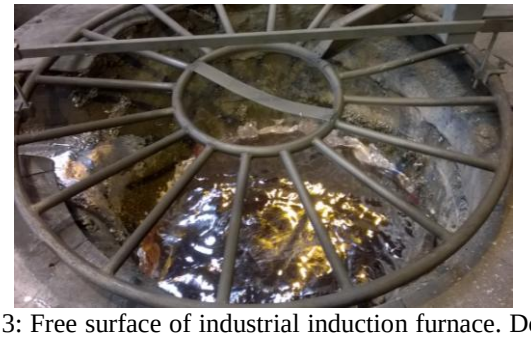

Fig. 3: Free surface of industrial induction furnace. Dome with large fluctuation (E1).

Fig. 4: Free surface of industrial furnace. Dome with small fluctuation (E2).

In the first case, the furnace is full with molten metal (Fig 3). In the second case, the furnace is filled to 2/3 of its capacity (Fig. 4). Experimentally, we observe strong fluctuations of the metal surface with full furnace configuration (E1), especially near the crucible wall. The surface of metal changes very little in the second case. Fig. 5 and Fig. 6 present numerical results with the temporal evolution (over a period of 6 s) of the dome profiles for the two experimental sets (E1 & E2). While for E1, we see large fluctuations along with an irregular profile deformation (especially near the crucible wall), for E2, we obtain a smooth profile deformation with relatively much smaller fluctuation amplitude. Fig. 7 presents the contact points on the crucible axis or side wall, extracted from these dome profiles. This figure confirms the stability of the metal surface in the second case.

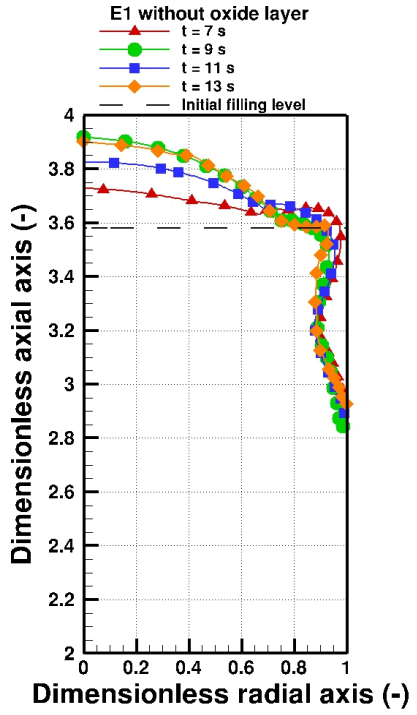

Fig. 5: Temporal evolution of dome profiles – E1.

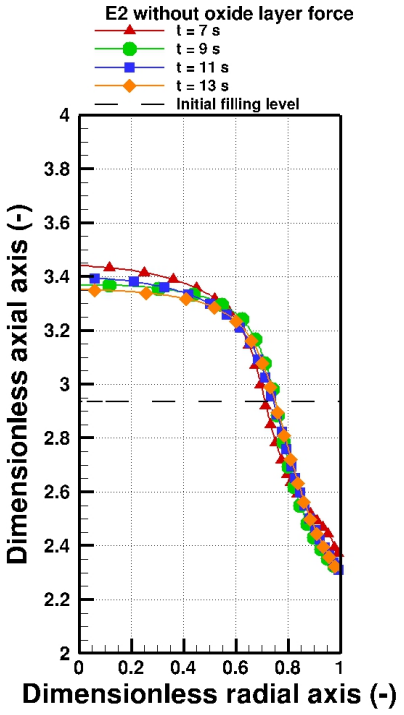

Fig. 6: Temporal evolution of dome profiles – E2.

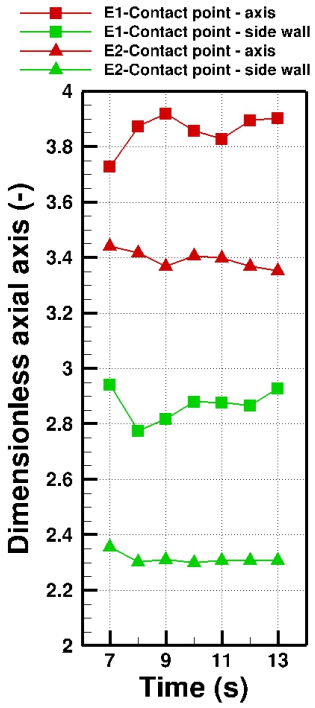

Fig. 7: E1&E2 temporal evolution of dome contact points.

Conclusion

A numerical tool to calculate the hydrodynamic in an induction furnace was developed. Validated with metal dome deformation measurements at a laboratory scale induction furnace using a 4 kg molten metal bath of aluminium, this model allows to find the tendencies observed experimentally on an industrial furnace (5 tons) with a more or less stable surface when the filling level varies. A more detailed validation of the model on an industrial scale with dome deformation measurements by telemetry is in progress.

Acknowledgment

This research work is supported by the French National Research Agency within the framework of the project ANR PRINCIPIA (2010-RMNP-0007).

References

[1] W. Schmitz, D. Trauzedell (2013), Casting plant and technology, 4, 12-19.
[2] A. Peel, P.-Y. Menet (2015), J. Manuf. Sci. Prod.; 15(1): 59-67.
[3] R. Stal, P. Hanley (2009), in Light Metals 2009, TMS-AIME, 627-630.
[4] M.W. Kennedy, J.A. Bakke, R.E. Aunes (2015), J. Manuf. Sci. Prod.; 15(1): 69-78.
[5] D. Shu, J. Wang, B. Sun (2015), J. Manuf. Sci. Prod; 15(1): 89-92.
[6] R. Fritzsch, M.W. Kennedy, S. Akbarnedjad, R.E. Aunes (2015), in Light Metals 2015, TMS-AIME, 929-935.
[7] R. Howitt, A.M. Peel (2004), WO 2004101199 A2 patent.
[8] Y. Delannoy, C. Alemany, K-I. Li, P. Proulx, C. Trassy (2002), Solar Energy Materials and Solar Cells 72/1-4, 69-75.
[9] A. Bansal, P. Chapelle, Y. Delannoy, E. Waz, P. Le Brun, J.P. Bellot (2015), in Light Metals 2015, TMS-AIME, 999-1004.